JOURNAL OF MARINE RESEARCH

The *Journal of Marine Research,* one of the oldest journals in American marine science, published important peer-reviewed original research on a broad array of topics in physical, biological, and chemical oceanography vital to the academic oceanographic community in the long and rich tradition of the Sears Foundation for Marine Research at Yale University.

An archive of all issues from 1937 to 2021 (Volume 1–79) are available through EliScholar, a digital platform for scholarly publishing provided by Yale University Library at https://elischolar.library.yale.edu/.

Requests for permission to clear rights for use of this content should be directed to the authors, their estates, or other representatives. The *Journal of Marine Research* has no contact information beyond the affiliations listed in the published articles. We ask that you provide attribution to the *Journal of Marine Research.*

Meridional transport in the Indian Ocean traced by coral radiocarbon

by Nancy S. Grumet[1], Thomas P. Guilderson[2,3] and Robert B. Dunbar[1]

ABSTRACT

Ocean circulation in the Indian Ocean is predominantly driven by the monsoon and is responsible for convergence along the equator. As a result, upwelling is primarily restricted to the western boundary where surface waters are anomalously depleted in ^{14}C. Here, we describe aspects of western boundary upwelling based on insights derived from the first coral radiocarbon time-series in the Indian Ocean. The absence of a distinct subannual pre-bomb Δ^{14}C signal suggests that open and coastal upwelling are negligible off the coast of Kenya. Instead, our results suggest that upwelling from the coast of Somalia and possibly Oman are the sources of the depleted seasonal Δ^{14}C signal. In contrast, the southern hemisphere subtropical gyre provides water enriched in ^{14}C. We demonstrate that the coral Δ^{14}C time-series is a tracer for meridional transport in the Indian Ocean. The Indian Ocean exhibits a shallow cross-equatorial overturning circulation cell. Our results demonstrate that the Kenyan coral radiocarbon record is responding to a western boundary limb of this cell, similar to that observed in other subtropical oceans. Therefore, while the majority of cross-equatorial transport is in the interior and eastern basin of the Indian Ocean, our results argue that the Somali Current is a distinct pathway for inter-hemispheric water mass exchange.

1. Introduction

The Indian Ocean is unique because it does not possess an equatorial upwelling regime. Instead upwelling is restricted to coastal areas of the northern hemisphere. In contrast, equatorial upwelling in the Pacific and Atlantic oceans occurs via subtropical cells. Within these cells, equatorward thermocline flow and coastal undercurrents play a major role in connecting the extratropical subduction regimes with tropical upwelling. Several recent studies (e.g., Schott and McCreary, 2001; Miyama *et al.,* 2002; Schott *et al.,* 2002) have proposed that the Indian Ocean contains a Cross-equatorial Cell (CEC) that is responsible for shallow (less than 500-m), meridional overturning circulation. The Indian Ocean CEC acts as a counterpart to the subtropical cells observed in the Pacific and Atlantic Oceans. Schott *et al.* (2002) describe the shallow cell as carrying cool thermocline water from

1. Department of Geological and Environmental Sciences, Stanford University, Stanford, California, 94305, U.S.A. *email: ngrumet@stanford.edu*
2. Center for Accelerator Mass Spectrometry, Lawrence Livermore National Laboratory, Livermore, California, 94551, U.S.A.
3. Also at the Department of Ocean Sciences, University of California, Santa Cruz, California, 95064, U.S.A.
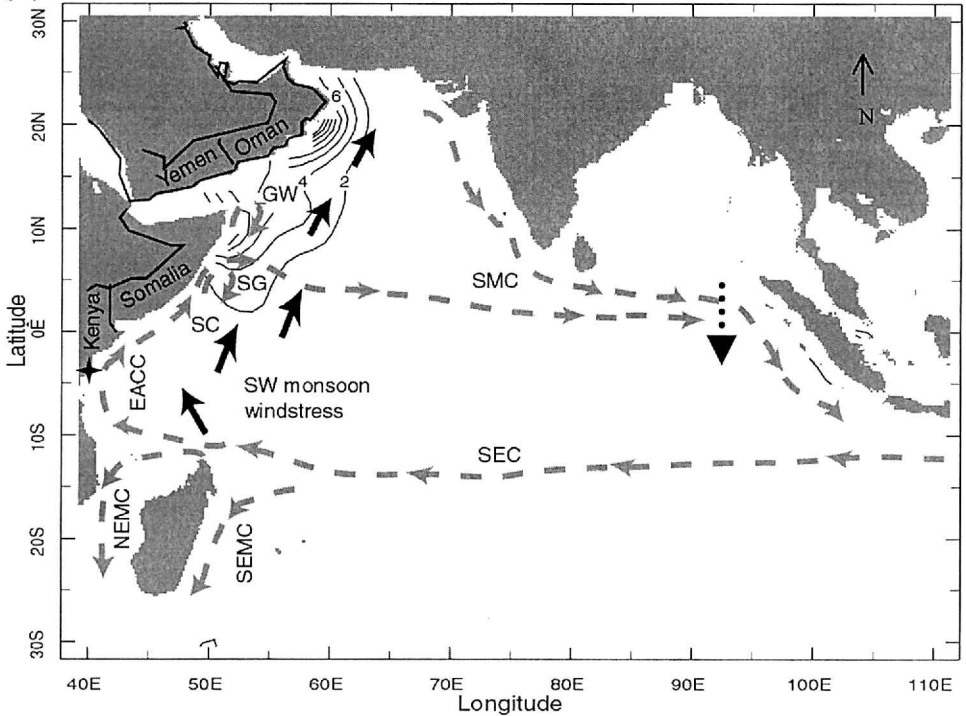
Figure 1. (a) Coral cores were collected by drilling massive colonies of *Porites lutea* off the coast of Kenya, designated by a star, at Malindi (3°14'S, 40°8'E), and Watamu (3°23'S, 39°52'E) Summer (July–Aug.–Sept.) surface (<10 m) nitrate concentrations are shown by contours intervals in μmol/l (Conkright *et al.,* 1998). Surface currents in the Indian Ocean during the SW monsoon: Somali Current (SC), East African Coastal Current (EACC), Southwest Monsoon Current (SMC), South Equatorial Current (SEC), and Northeast and Southeast Madagascar Currents (NEMC and SEMC). Upwelling regions are associated with the Southern Gyre (SG) and Great Whirl (GW). Thick black arrows indicate predominant SW monsoon wind stress from the US National Centers for Environmental Prediction (NCEP) climatology for July. Thick black stippled arrow indicates southward Ekman transport on both sides of the equator (modified from Tomczak and Godfrey, 1994; Schott and Fischer, 2000; Schott and McCreary, 2001). (b) Winter (Jan.–Feb.–March) surface (<10 m) nitrate concentrations are shown by contours intervals in μmol/l (Conkright *et al.,* 1998). Surface currents in the Indian Ocean during the NE monsoon: Somali Current (SC), East African Coastal Current (EACC), North Equatorial Current (NEC), South Equatorial Counter Current (SECC), South Equatorial Current (SEC), and Northeast and Southeast Madagascar Currents (NEMC and SEMC). Thick black arrows indicate predominant NE monsoon wind stress from the US National Centers for Environmental Prediction (NCEP) climatology for January. Thick black stippled arrow indicates northward Ekman transport on both sides of the equator (modified from Tomczak and Godfrey, 1994; Schott and Fischer, 2000; Schott and McCreary, 2001).

(b)
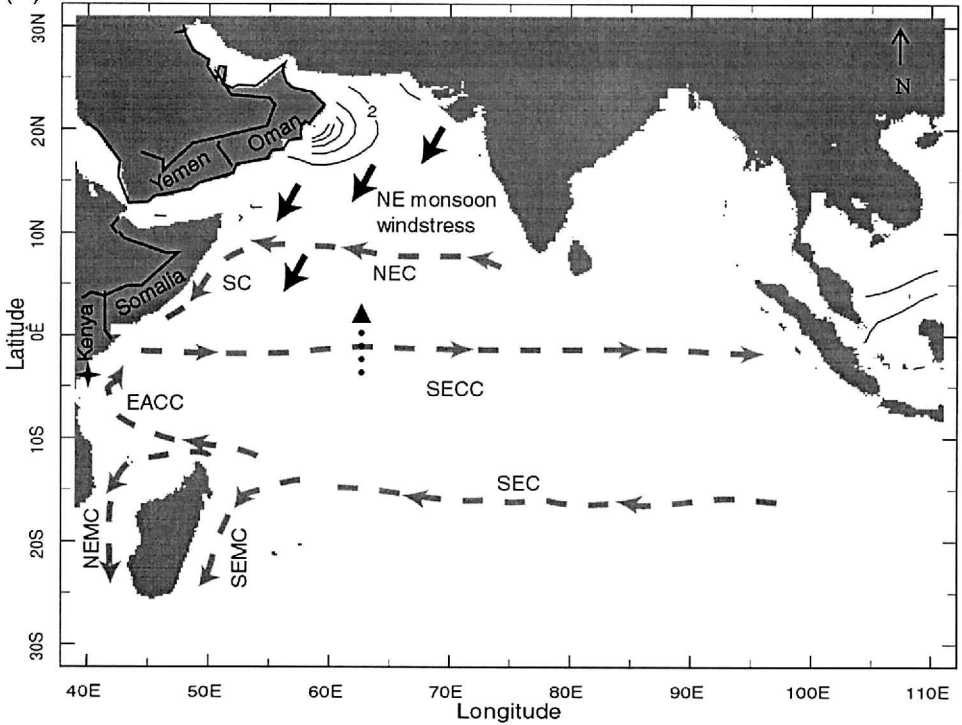
subduction regions in the southern, subtropical Indian Ocean via the South Equatorial Current (SEC), East African Coastal Current (EACC), and the Somali Current (SC) to the upwelling regions off Somalia and Arabia, with return surface flow across the equator in the interior ocean and eastern boundary by Ekman flow (Fig. 1). However, the contribution of possible return flow along the western boundary current has not yet been considered. In this paper, we investigate the role of the wintertime SC in transporting upwelled water across the equator during the Northeast (NE) Monsoon. In this study we present the first continuous, bimonthly resolved radiocarbon time-series (1947–1987) measured in a coral from the Indian Ocean, and explore the fidelity of this record as a tracer for meridional circulation.

2. Background

a. Physical oceanography

The influence of the monsoons on the northern Indian Ocean is seen in the reversals of the surface circulation and in the temperature and salinity conditions of the surface waters extending to 10–20S. The northern and equatorial Indian Ocean circulation is especially complex with large seasonal variations and reversals in major current systems (Table 1).

Table 1. Seasonal designation and terminology used to describe the flow direction of the Somali
Current (SC) during the monsoon cycle.

	Southwest monsoon	Northeast monsoon
Season	boreal summer	boreal winter
SC flow direction	northward	southward

For example, as a response to prevailing southwesterly flow in the lower troposphere
during the Southwest (SW) Monsoon, a northward flowing EACC is strongly developed as
a continuation of the SEC and contributes to the progression of the northward flowing SC
and the Southwest Monsoon Current (SMC) to the east (Fig. 1a). Recognized as the
western boundary current that causes structural readjustment in the baroclinicity down to
1000 m, the SC is responsible for strong upwelling along the northern coasts of Somalia
and Oman and the appearance of the Southern Gyre (SG) and Great Whirl (GW) during the
SW monsoon (Luther, 1999). Surface water flow during the SW monsoon is predominantly
in an eastward direction.

   In contrast, during the NE monsoon, northeasterly winds cause surface waters north of
the equator to flow to the west or southwest comprising the North Equatorial Current
(NEC) (Rao and Griffiths, 1998) (Fig. 1b). At the equator, south-flowing water off the
coast of Somalia together with the northflowing EACC feed the South Equatorial Counter
Current (SECC), which moves eastward across the Indian Ocean between 0° and 8S
(Schott and McCreary, 2001). Throughout the monsoon cycle the Southeast Trade Winds
dominate south of the equator and the SEC flows westward at approximately 10–15S and
bifurcates to form the Northeast and Southeast Madagascar Currents (NEMC and SEMC).

   The wind-driven monsoon circulation described above is responsible for linking the
subduction regions of the southern, subtropical Indian Ocean to the upwelling regions off
Somalia and Arabia. As mentioned earlier, this process has been termed the Cross-
equatorial Cell (Schott and McCreary, 2001; Miyama *et al.,* 2002; Schott *et al.,* 2002).
Subducted waters, primarily restricted to the Southern Hemisphere, are advected westward
in the SEC and then northward in the EACC (Schott and McCreary, 2001; Miyama *et al.,*
2002). Upon crossing the equator, this subsurface flow feeds into the SC, eventually
upwelling in the Northern Hemisphere and joining the CEC. Miyama *et al.* (2002)
demonstrate that the majority of return surface flow across the equator is near the eastern
boundary.

b. Radiocarbon as a tracer for water mass circulation

   The analysis of transient anthropogenic tracers in the world's oceans, such as radiocar-
bon (^{14}C), has greatly enhanced our understanding of deep thermohaline circulation and
ventilation of subthermocline waters (e.g., Rhein *et al.,* 1995; Jenkins, 1996). For example,
surface ^{14}C variability in the Galapagos is influenced by the vigor of upwelling and by the
origin of upwelling water (Guilderson and Schrag, 1998). The deep ocean is depleted in

^{14}C relative to the surface ocean due to the long residence time of deep ocean water, which allows for significant ^{14}C decay ($t_{1/2}$ = 5730 yrs). In contrast, the surface ocean is enriched in ^{14}C as a result of air-sea gas exchange processes. Nuclear weapon testing in the 1950s produced an excess of ^{14}C that has augmented this difference between surface and deep ocean concentrations. This enrichment makes the distribution of ^{14}C very sensitive to vertical mixing and a useful ocean circulation tracer.

Surface and subsurface measurements of radiocarbon isotope (Δ^{14}C), such as that conducted by Geochemical Ocean Section Study (GEOSECS), Indien Gaz Ocean (INDIGO), and World Ocean Circulation Experiment (WOCE) programs have improved our understanding of intense monsoon driven upwelling that occurs off Somalia and the Arabian Coast (e.g., Broecker *et al.,* 1985; Bard *et al.,* 1989; Ostlund and Grall, 1991). While results from these programs have been extremely valuable, vertical profiles are subject to temporal aliasing since the measurements represent a "snapshot" of conditions. Such snapshots may be augmented with time-series developed from radiocarbon records from tropical corals.

Corals incorporate dissolved inorganic carbon from the surrounding seawater into their skeleton. As a result, radiocarbon measurements from banded corals have been shown to represent radiocarbon levels of dissolved inorganic carbon (DIC) from neighboring surface waters (Druffel and Linick, 1978; Druffel, 1982). Coral Δ^{14}C reflects the seawater ^{14}C/^{12}C ratio at the time of precipitation and the accreted aragonite provides an unaltered record of ^{14}C/^{12}C ratios present in seawater (e.g., Druffel, 1989; Brown *et al.,* 1993; Guilderson *et al.,* 1998, 2000). Therefore, radiocarbon levels can be determined for the past 100 years or more in many regions of the tropics and sub-tropics where corals grow. In addition, sea surface temperature (SST) records reconstructed from oxygen isotope ratios (δ^{18}O) can be correlated to coral Δ^{14}C records in order to estimate the relative influence that atmospheric exchange processes and surface circulation have on determining the ^{14}C content of equatorial waters (Druffel, 1987). Using these records, scientists have uncovered evidence of past vertical changes in surface-subsurface mixing and horizontal current shifts. These records also provide boundary constraints used to test parameterization of ocean dynamics in circulation models (e.g., Rodgers *et al.,* 1997, 2000).

3. Methods

Cores collected from massive hermatypic corals *Porites lutea* off the coast of Kenya were sampled to assess seasonal and spatial variability in the coral oxygen isotope (δ^{18}O) and Δ^{14}C signal (Fig. 1). The 63-cm coral core used to construct the record presented here was collected in August 1996 from Watamu, Kenya (3°23'S, 39°52'E). A low speed drill was used to extract aragonite powder every 2-mm (~6 samples per year) for Δ^{14}C analysis at the Center for Accelerator Mass Spectrometry (CAMS) at Lawrence Livermore National Laboratory (LLNL). Radiocarbon results are reported as Δ^{14}C‰ as defined by Stuiver and Polach (1977). These results include a minor background correction using a calcite standard and are δ^{13}C and age corrected. Concurrent analysis of an in-house standard
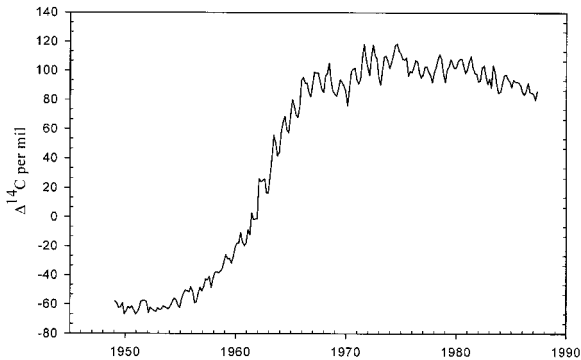
Figure 2. Bimonthly Watamu coral $\Delta^{14}C$ (in per mil ‰) time-series from 1947–1987. The pre-bomb interval is defined from 1947 to 1955 when ^{14}C variability is due to natural ^{14}C variation and averages -60 ± 3.7‰. Post-bomb coral $\Delta^{14}C$ values, defined as after 1955, respond dramatically to atmospheric nuclear bomb testing in the late 1950s and continue to increase until the mid-1970s.

yielded an external error of ± 3.7‰ (1σ, normalized to "fraction modern" (Fmodern) = 1.0; $n = 23$). Samples were collected every 1-mm for $\delta^{18}O$ analysis (~12 samples per year) and were analyzed at the Stanford University Stable Isotope Laboratory. Approximately 15% of the samples were replicated, yielding an average standard deviation of less than 0.05‰ for $\delta^{18}O$ and 0.12‰ for $\delta^{13}C$. All results are reported relative to the international V-PDB (Vienna Pee Dee Belemite) standard (Coplen, 1994). A detailed discussion of the methodology is given in Grumet *et al.* (2002).

Well-developed annual density bands and minimum and maximum $\delta^{18}O$ values were used to define the chronology (Grumet *et al.,* 2001). Instrumental SST records indicate that the maximum (minimum) temperature off the coast of Kenya occurs in March/April (July/August). Accordingly, the minimum and maximum coral $\delta^{18}O$ values were assigned the corresponding calendar date. Samples in between these points were linearly interpolated in order to construct a sub-annually resolved age model. The assigned calendar months also show a strong correspondence to changes in density. The minimum $\delta^{18}O$ values in April coincide with high-density bands. As indicated by instrumental records, this is the warmest time of the year, when calcification exceeds extension (linear growth), resulting in the formation of high-density bands (Highsmith, 1979).

4. Results

According to our age model, the Watamu bimonthly $\Delta^{14}C$ time-series covers the period from 1947–1987 with an absolute year-month data assignment error of less than 3–4 months. The resulting time-series captures the surface ocean's response to the input of excess ^{14}C from atmospheric nuclear bomb testing (Fig. 2). Coral radiocarbon levels begin to respond to atmospheric testing in the late 1950s. According to this dramatic change in slope, we define the pre-bomb interval as 1947 to 1955. During this interval, radiocarbon
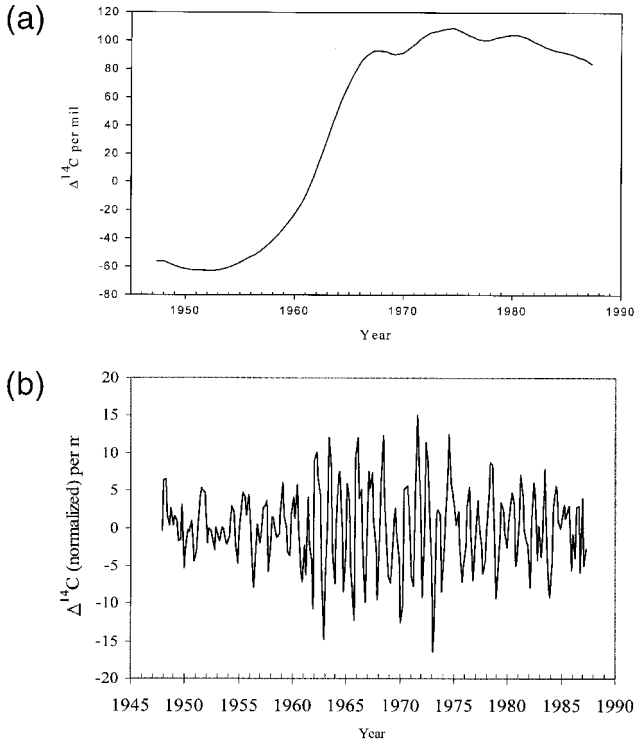
Figure 3. (a) Long-term Watamu coral Δ^{14}C (in per mil ‰) trend from 1947–1987. The time-series was developed using Singular Spectral Analysis to isolate the leading components attributed to tenfold increase in atmospheric ^{14}C. The coral Δ^{14}C peak is approximately 10 years after the atmospheric maximum value in 1963. (b) De-trended bimonthly Watamu coral Δ^{14}C (in per mil ‰; normalized) time-series illustrating sub-annual to annual variability from 1947–1987. The seasonal variability reflects the competition between air-sea exchange processes and vertical/horizontal mixing within the ocean.

levels average -60‰ (uncorrected for a -10‰ fossil fuel effect) and yield a standard deviation of ±4‰. The sub-annual range, calculated as the difference between the minimum and maximum Δ^{14}C value within a given year, is less than 6‰ during the pre-bomb interval (Grumet *et al.*, 2002).

The post-bomb coral Δ^{14}C record is characterized by a maximum value (121‰) in the mid-1970s. This peak occurs approximately 10 years after the 1963 atmospheric bomb radiocarbon peak (Nydal, 2000). Singular Spectrum Analysis (SSA-Toolkit; Dettinger *et al.*, 1995; Vautard *et al.*, 1992) was used to identify the long-term Δ^{14}C trend (Fig. 3a) that captures the influx of bomb-laden ^{14}C from the atmosphere into the upper ocean. This long-term trend was then subtracted from the original time-series in order to isolate the annual to subannual record, referred to as the de-trended time-series (Fig. 3b). Applying a high-pass filter with a cut-off period of 6 years yields an equivalent time-series to the SSA
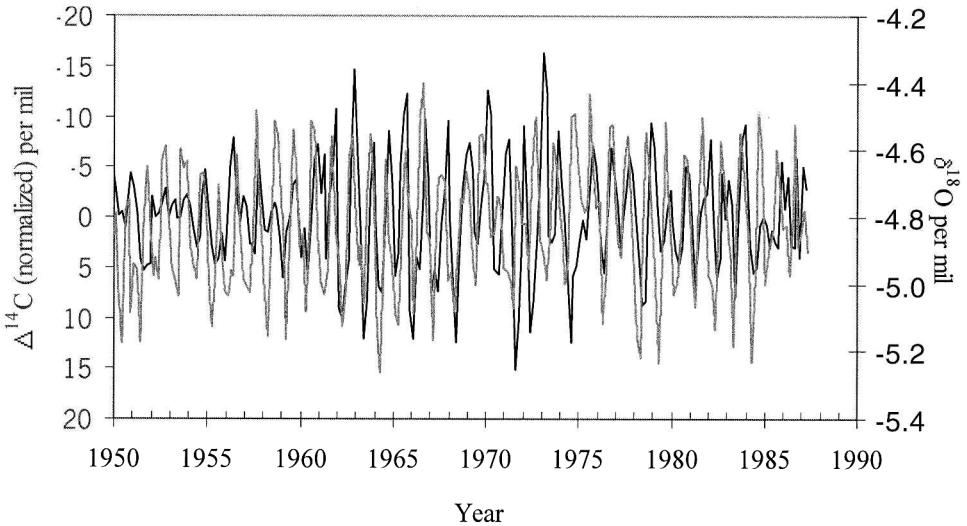
Figure 4. De-trended Watamu $\Delta^{14}C$ (normalized) and $\delta^{18}O$ bimonthly time-series from 1950 to 1987. The enriched $\delta^{18}O$ appears to lead the depleted $\Delta^{14}C$ by 1 to 2 time steps. This would result in the $\delta^{18}O$ signal leading the $\Delta^{14}C$ signal by 3 to 4 months. The enriched $\delta^{18}O$ signal (indicative of colder sea-surface temperatures) peaks in July–August, while the most depleted $\Delta^{14}C$ signal (indicative of oceanic mixing) appears to dominate the months of Nov.–Jan. (note: $\Delta^{14}C$ axis is inverted).

residual time-series ($r = 0.98$). The sub-annual range increases in the early 1960s and throughout the early 1970s to over 25‰. In the latter part of the record, from 1977 to 1986, the sub-annual range decreases to less than 15‰.

The strongest phase relationship between the de-trended $\Delta^{14}C$ time-series defined by SSA and the Watamu bimonthly $\delta^{18}O$ time-series is a negative lag of approximately 1 to 2 time-steps (Fig. 4). According to our sampling procedure of 2-mm and age assignment, this would result in the enriched $\delta^{18}O$ seasonal signal leading the depleted $\Delta^{14}C$ seasonal signal by 3 to 4 months. Sorting the bimonthly normalized coral $\Delta^{14}C$ data into a "depleted" and an "enriched" signal (using the analytical error of ±3.7‰ as a point of separation), illustrates that the most depleted $\Delta^{14}C$ signal occurs in the Nov.–Dec. while the most enriched $\Delta^{14}C$ signal occurs in May–June. In other words, the most positive $\delta^{18}O$ (cool/dry) seasonal signal occurs in July–August (Grumet *et al.,* 2001), while the most depleted $\Delta^{14}C$ signal occurs during the months between Nov.–Jan. In contrast, enriched $\Delta^{14}C$ values occur in May–June, coinciding with the onset of the SW monsoon.

GEOSECS and INDIGO surface $\Delta^{14}C$ values are available for comparison with our coral record. We chose hydrographic sites that were within $10°$ latitude and longitude of the Watamu coral site. GEOSECS cruise data collected in the January 1977–78 from stations 419, 420 and 421 reveal a surface $\Delta^{14}C$ value of 94‰ (Stuiver and Ostlund, 1983), while the coral value at this time is 98‰. Similarly, INDIGO cruise data collected in the

Table 2. Interbasin comparison between coral Δ^{14}C (in per mil ‰) time-series in the Pacific Ocean and Indian Ocean. The equatorial sites, Galapagos (90W) and Nauru (0.5W, 166E) tend to yield a post-bomb maximum almost 10 year after the subtropical sites, Rarotonga (21S, 159W), French Frigate Shoals (24N, 166W), and Fiji (18S, 180E). The Watamu (3S, 39E) site represents an intermediate site between the Pacific tropical and subtropical end-members (see Fig. 6 for map).

	Galapagos[1]	Nauru[2]	Rarotonga[3]	French Frigate Shoals[4]	Fiji[5]	Watamu[6]
Pre-bomb average[+]	−80	−58	−52	−50	−60	−60
Maximum	60	137	153	189	138	121
Year	1985	1983	1972	1971	1973–4	1974
	*70 1993					

[1]Guilderson and Schrag, 1998; [2]Guilderson *et al.,* 1998; [3]Guilderson *et al.,* 2000; [4]Druffel, 1987; [5]Toggweiler *et al.,* 1991; [6]this study.
*WOCE 1995 cruise data.
[+]Uncorrected for fossil fuel effect.

March–April of 1986 from stations 38, 43, and 45 capture a surface Δ^{14}C value of 85‰ (Ostlund and Grall, 1991), while the coral value at this time is 92‰. Analytical error for radiocarbon in surface water measured from the hydrographic cruises discussed above is approximately ±4‰. Within analytical error, the coral correctly records this small Δ^{14}C trend between 1977 and 1986.

An interbasin comparison between the Watamu Δ^{14}C time-series and those derived from the Pacific Ocean is outlined in Table 2 and illustrated in Figures 5 and 6. Pre-bomb coral Δ^{14}C at subtropical sites in the Pacific, Fiji (Toggweiler *et al.,* 1991), Rarotonga (Guilderson *et al.,* 2000), and French Frigate Shoals (Druffel, 1987) average −54‰ and are elevated compared to the equatorial site, Galapagos, which displays a pre-bomb average of −80‰ (Guilderson and Schrag, 1998). The post-bomb peak at the subtropical sites occurs approximately 10 years after the atmospheric peak, while the tropical Pacific sites do not exhibit a maximum bomb-peak until at least the 1980s, if not later. In comparison to these results (Table 2), the Watamu Δ^{14}C coral time-series peaks in 1972 and yields a pre-bomb average of −60‰.

5. Discussion

The long term trend (Fig. 3a) identified in the Watamu Δ^{14}C record is consistent with other reports documenting the influx of atmospheric bomb ^{14}C into the ocean during the mid to late 1950s (Nydal, 2000). Our comparison with hydrographic data suggests that the Watamu coral is accurately recording surface water radiocarbon conditions. The 10 year delay in the Watamu Δ^{14}C peak, relative to the atmospheric peak, is believed to represent the time required for isotopic equilibrium (Broecker and Peng, 1982; Druffel and Suess, 1983; Druffel, 1987). An interbasin comparison between coral Δ^{14}C time-series reveals
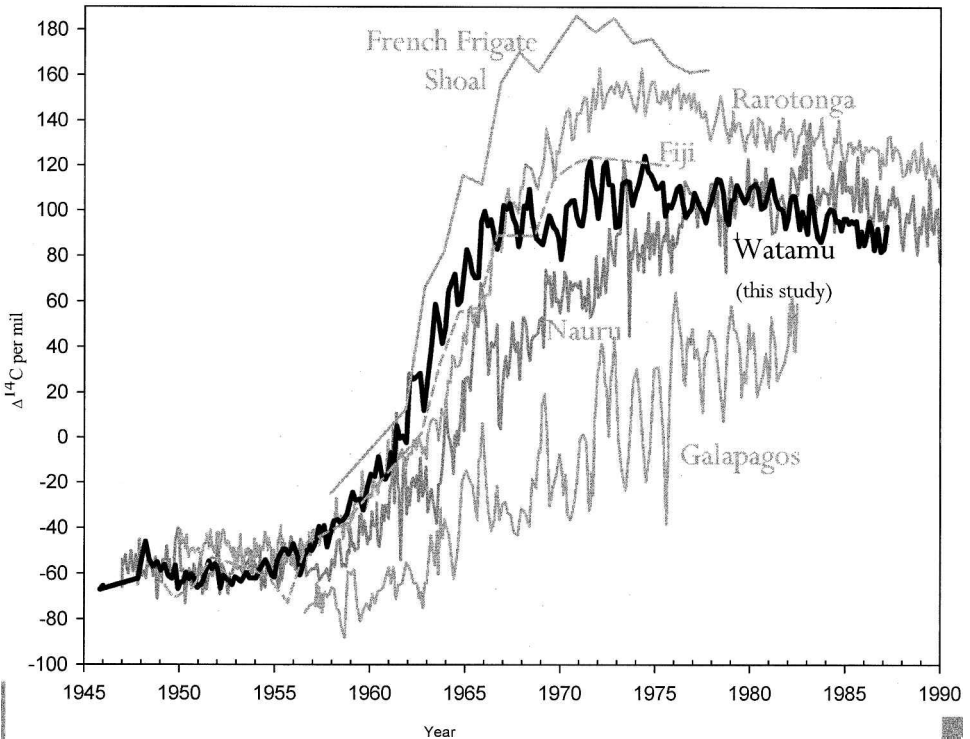
Figure 5. Interbasin comparison between radiocarbon time-series developed from the Pacific and Indian Oceans. The equatorial sites, Galapagos (90°W) and Nauru (0.5W, 166E) tend to yield a post-bomb maximum almost 10 year after the subtropical sites, Rarotonga (21S, 159W), French Frigate Shoals (24N, 166W), and Fiji (18S, 180E). The Watamu (3S, 39E) site represents an intermediate site between the Pacific tropical and subtropical end-members.

differences in air-sea exchange rates and horizontal and vertical mixing between the Pacific and Indian Ocean equatorial and subtropical sites, as illustrated by differences in pre-bomb averages and in the timing and magnitude of the post-bomb peak (Fig. 5). The delayed maximum bomb-peak observed in the equatorial Pacific coral records is a consequence of both the ventilation time of the tropical Pacific thermocline, and entrainment of deeper subthermocline waters (Guilderson *et al.,* 1998; Guilderson and Schrag, 1998). Chronologically, the Watamu post-bomb peak behaves like a subtropical site yielding a maximum $\Delta^{14}C$ value that lags the atmospheric peak by 10 years. Yet the magnitude of the post-bomb peak and the slow overturning of the bomb signal are comparable to the tropical sites. The Watamu post-bomb time-series represents an intermediate site between the Pacific tropical and subtropical end-members. This result suggests that a different mechanism, as discussed later, is responsible for distributing water between the tropics and extratropics in the western equatorial Indian Ocean.

As Schott and McCreary (2001) explain, the Southeast Trades do not cross the equator,
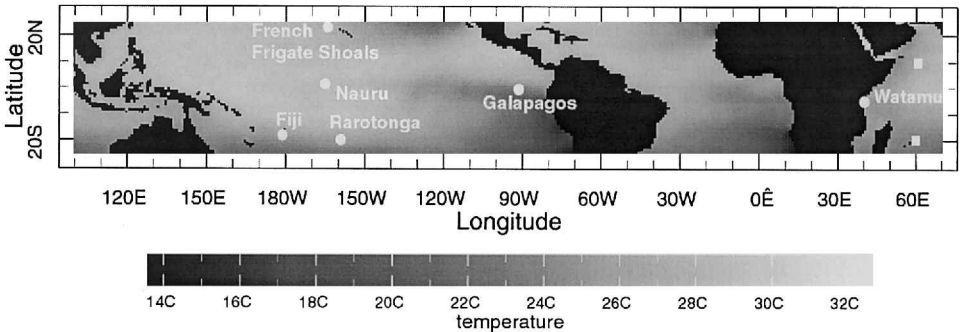
Figure 6. Tropical Pacific, Atlantic and Indian Ocean mean seasonal (June–July–August) sea surface temperature (Conkright *et al.*, 1998). Coral site locations discussed in the text, Figure 5 and Table 2 are demarked by circles and names. GEOSECS, WOCE and INDIGO hydrographic sites used to calculate an Arabian Sea and subtropical gyre component for the end-member mixing calculation are centered at 15/60E and 20/60E, respectively and are designated by squares.

inhibiting equatorial divergence; hence, upwelling does not occur along the equator in the Indian Ocean. In agreement, our results illustrate a pre-bomb seasonal gradient indistinguishable from the analytical error (± 4‰), suggesting that local upwelling is relatively weak or negligible off the equatorial coast of Kenya (Grumet *et al.*, 2002). Relative to regional pre-bomb Δ^{14}C values in the western Indian Ocean, our results indicate ^{14}C enrichment off the coast of Kenya. Between 1947–1955, the bimonthly Watamu Δ^{14}C record averages -51‰ (corrected for a -10‰ fossil fuel effect). Southon *et al.* (2002) estimate a regional Δ^{14}C mean of -73‰ in the western Arabian Sea and a mean of -66‰ in the tropical southwestern Indian Ocean. Unlike pre-bomb values south of the equator near Seychelles and Madagascar, our pre-bomb values are enriched by more than 10‰. Southon *et al.* (2002) suggest that the influence of monsoon-driven upwelling is propagated throughout the western Indian Ocean by the major current systems, especially the SEC. Alternatively, upwelling near Saya de Malha Bank observed from numerical modeling studies (Ji and Luther, 1999; Woodberry *et al.*, 1989), could influence surface Δ^{14}C values near the Seychelles and Madagascar.

The phase relationship between the Watamu δ^{18}O and Δ^{14}C seasonal signals lends further support to the notion that highly localized vertical advection is not responsible for the depleted Δ^{14}C seasonal signal. The post-bomb record depicts depleted values in Nov.–Jan., while seasonally elevated Watamu δ^{18}O values occur in July–August, the coldest season (Grumet *et al.*, 2001). In contrast, Δ^{14}C values are the most positive in May–June, marking the onset of the SW monsoon. The coldest temperatures occur in the summer months as a result of evaporative cooling due to the southwesterly winds during the SW monsoon. If monsoon-induced local, vertical mixing were responsible for the seasonally depleted Δ^{14}C values, we would expect the bimonthly δ^{18}O and Δ^{14}C signal to be anti-correlated with a zero lag. The only time this is true is between 1957–1972.

However, because the $\Delta^{14}C$ signal is not steady state, the phase relationship changes over time. For the entire record, the depleted $\Delta^{14}C$ seasonal signal lags the enriched $\delta^{18}O$ seasonal signal by 3 to 4 months. Binning the data reveals a predominant depleted $\Delta^{14}C$ signal during the winter months. Therefore, we argue that local vertical mixing cannot be the primary mechanism driving the seasonal coral $\Delta^{14}C$ signal.

Based on these results, we suggest that upwelling from the coast of Somalia and possibly Oman are the sources of depleted seasonal $\Delta^{14}C$ signal. Most high productivity areas are found in upwelling regions, generally situated at western margins of the continents (e.g., Peru, Gulf of California, and Southwest Africa). An exception to this is provided by the monsoon-induced upwelling system in the northern and especially northwestern Indian Ocean. Open-ocean upwelling occurs as a consequence of Ekman pumping which is driven by strong positive windstress curl, and coastal ocean upwelling which is driven by the offshore deflection of surface waters by Ekman transport. The effect of upwelling is to deliver nutrients and relatively depleted $\Delta^{14}C$ to the upper water column. These surface waters are also characterized by lower anthropogenic CO_2 (Goyet *et al.,* 1999). Significantly depleted surface $\Delta^{14}C$ values measured from hydrographic data characterize the upwelling conditions in this region (Stuiver and Ostlund, 1983; Ostlund and Grall, 1991; Key *et al.,* 2002a). Another possible source of depleted $\Delta^{14}C$ is a region of open-ocean upwelling at 5–10S (Schott and McCreary, 2001). While there is satellite imagery of ocean color indicating phytoplankton blooms in this area (Murtugudde *et al.,* 1999), there is little instrumental data documenting the strength and/or existence of upwelling. Furthermore, since upwelling in this region supposedly occurs during the NE monsoon due to cyclonic wind stress, Ekman transport south of the equator is northward this time of year (Fig. 1b). Therefore, as a result of open-ocean upwelling, depleted $\Delta^{14}C$ would be advected northward and eventually eastward within the SECC, away from the coast of Kenya. Dynamically, it is difficult to accept that open-ocean upwelling at 5–10°S is the source of depleted $\Delta^{14}C$ off the coast of Kenya. Instead, we argue that the upwelling regions in the Arabian Sea are the most likely sources of depleted $\Delta^{14}C$ that bathe the surface waters off the coast of Kenya.

To estimate the proportion of Arabian Sea waters off Watamu we have utilized a simple two-end-member mixing model and the constraints imposed by measurements during GEOSECS, INDIGO, and WOCE. GEOSECS and INDIGO data were collected during the late winter/early spring in 1978 and 1986, respectively. From stations centered at 15N/60E and 20S/60E, we characterized an Arabian Sea and gyre component, respectively (Fig. 6). Using $\Delta^{14}C$ within the mixed layer (less than 50 m), GEOSECS Arabian Sea and gyre waters were 128‰ and 90‰ and a corresponding coral value of 98‰; similarly, INDIGO Arabian Sea and gyre waters were 116‰ and 80‰ and a correspond to a coral value of 92‰. These values yield an Arabian Sea component of 80% and 70% during the respective winter/early spring snapshots.

Using a similar approach, 1995 $\Delta^{14}C$ WOCE Arabian Sea and gyre waters were 66‰ and 44‰. Our coral record ends in 1987, therefore the WOCE station at 2.7S/56.4E was

used as "coral" value, corresponding to 57‰. In comparison to the GEOSECS and INDIGO data, the WOCE data yield an Arabian Sea component of only 40%. The WOCE data were collected in the late spring and throughout the summer, coinciding with the onset and strengthening of the SW monsoon. Thus, the decrease in the Arabian Sea component expressed in the WOCE end-member calculation reflects a weaker contribution from the Arabian Sea. Thus the majority of water influencing the coral site during the SW monsoon is from the south. In contrast, the GEOSECS and INDIGO data illustrate that the NE monsoon is characterized by a greater contribution from the Arabian Sea.

The most plausible mechanism for transporting upwelled, depleted $\Delta^{14}C$ surface water to the coast of Kenya is the wintertime SC during the NE monsoon. Based on an array of moored current meters deployed in the northern inflow region of the Somali Current during 1995–1996, Schott and Fischer (2000) show that during the NE monsoon, the SC flows equatorward south of 6–8N. However, the region around our coral site is extremely complex. The upper-layer flow of the SC is southward during the NE monsoon but is eventually forced eastward when these waters meet the EACC at 2–4°S, forming a confluence of water to supply the SECC (Fig. 1b) (Duing and Schott, 1978; Johnson *et al.,* 1982). As discussed earlier, Kenyan pre-bomb $\Delta^{14}C$ values are enriched relative to sites around Mauritius, northern Madagascar and Seychelles (Grumet *et al.,* 2002; Southon *et al.,* 2002). This comparison suggests that the influence of depleted $\Delta^{14}C$ water transported within the SEC is limited to regions south of 3 to 4S. Thus, it appears that our coral site is slightly north of this confluence.

To further investigate the proposed mechanism of transport, we used drifter trajectory output from the Japan Marine Science and Technology Center (JAMSTEC) general circulation model (GCM) (Fig. 7). The JAMSTEC GCM has a horizontal resolution of 0.25° and 55 vertical layers. The model is driven from initial state at rest with annual average temperature and salinity of Levitus (1982) climatology. After a 2 year initial spin-up stage, seasonal variability is driven by monthly climatologies from the last state of the initial spin-up (Ishida *et al.,* 1998; Miyama *et al.,* 2002). Tracked forward in time and at a depth of 10 m using the seasonally changing velocity fields, Miyama *et al.* (2002) demonstrate that drifters released in January remain north of the equator until the following summer when the majority of drifters cross the equator near the eastern boundary. The exception to this model scenario is for drifters that become entrained into the wintertime SC during the NE monsoon and are advected southward and cross the equator at the western boundary (Fig. 7). Indeed, as Miyama *et al.* (2002) discovered, the CEC surface branch can cross the equator at all longitudes and our results provide empirical documentation of such western boundary flow.

In comparison to the northern hemisphere, subduction occurs dominantly in the southeastern subtropical Indian Ocean (Zhang and Talley, 1998; Karstensen and Quadfasel, 2002). The water column in the subtropical gyre is relatively stable and surface waters reside sufficiently long to absorb a significant amount of ^{14}C from the atmosphere. As a result of downwelling in the subtropics, the Indian Ocean yields a maximum $\Delta^{14}C$
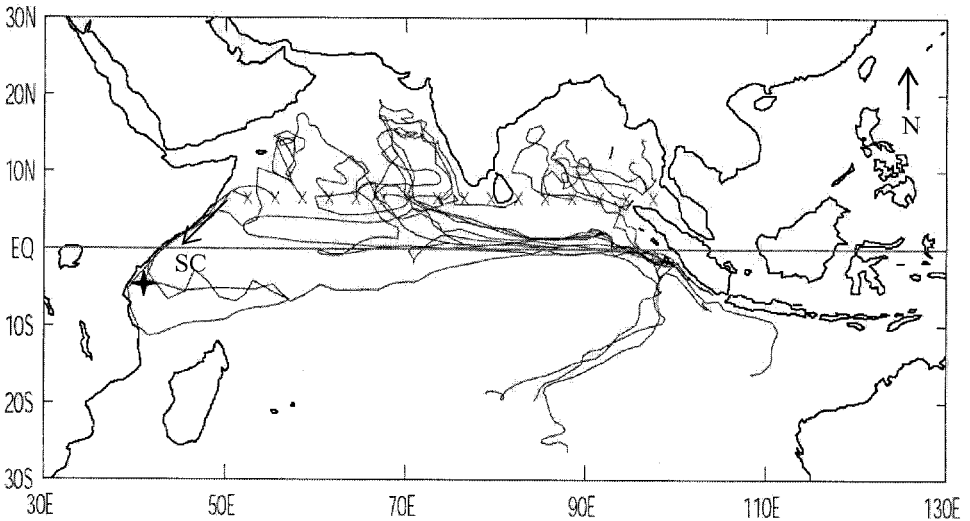
Figure 7. Drifter trajectories at a depth of 10-m tracked forward using the seasonally changing velocity field of the JAMSTEC model solution with vertical component = 0. Initial points (crosses) were released on January 1 and tracked forward in time for 12 months. The Watamu coral site is designated by a star and the Somali Current during the NE monsoon is indicated by an arrow.

inventory centered between 20°S and 40°S (Stuiver and Ostlund, 1983; Bard *et al.,* 1988). The subducted water, along with Indonesian Throughflow water, is advected westward within the SEC and divides near 17S into the Madagascar Currents (Swallow *et al.,* 1988; Fig. 1a and 1b). Eventually, those water masses that pass the northern tip of Madagascar merge into the EACC and from May to September these waters feed the northward flowing Somali Current. This observation is supported by trajectory results from five independent ocean models (Miyama *et al.,* 2002). The low salinity waters off Somalia identify it as water from the southern hemisphere (Fischer *et al.,* 1996). Schott *et al.* (2002) estimate that the SW monsoon mean of the cross-equatorial flow is 22 Sv. Therefore, we propose that advection of enriched ^{14}C from the subtropical gyre is responsible for seasonally elevated coral $\Delta^{14}C$ off the coast of Kenya during the SW monsoon.

We are confident that the meridional circulation described herein persisted during the pre-bomb period. However, since $\Delta^{14}C$ is a transient tracer there is an inherent time varying gradient in the surface water concentrations. The lateral (e.g., north to south) surface water $\Delta^{14}C$ gradient was weaker prior to nuclear bomb testing. Polynomial reconstruction of pre-nuclear $\Delta^{14}C$ surface levels from Indian Ocean GEOSECS and INDIGO stations from the coast of Somalia and from 20S/50–60E average −59‰ and −52‰, respectively (Bard *et al.,* 1988). Based on these reconstructions, the pre-bomb lateral gradient was relatively weak, approximately 7‰ over 20° of latitude. In contrast, according to INDIGO cruise data a lateral gradient of approximately 35‰ existed in 1986

(Ostlund and Grall, 1991). We propose that the pre-bomb Watamu coral Δ^{14}C record is insensitive to mixing with upwelled water from Oman and Somalia due to the weak lateral gradient; only when the gradient is sufficient (e.g., post-bomb) does the Watamu record capture sub-annual variability. Hence, our sub-annual coral Δ^{14}C record is most useful during the post-bomb period when the lateral gradient is amplified by nuclear bomb testing.

Assuming our proposed mechanism of transport is accurate, we can interpret the seasonal to interseasonal variability in the Watamu Δ^{14}C record as a tracer for meridional transport. We suggest that the large seasonal amplitude in the 1970s reflect the surface waters responding more quickly than the undercurrent to the invasion of the bomb-laden Δ^{14}C, especially in the subtropical gyre. The modulated seasonal amplitude observed later in the record might reflect mixing with the undercurrent that is now "younger." In other words, as the bomb Δ^{14}C signal penetrates the upper water column, the oceanic Δ^{14}C maximum is below the surface. This pattern is observed in 1995 WOCE data that show upwelled waters at low latitudes in the Pacific with a higher bomb radiocarbon levels than during the 1978 GEOSECS survey (Key *et al.,* 2002b). Therefore, our results reveal that sufficient time has occurred to allow mixing (between the surface and subsurface) to compete with air-sea exchange processes in determining the surface ocean Δ^{14}C signature in the western Indian Ocean.

6. Conclusion

In this study we have shown that radiocarbon measured in a coral collected off the coast of Kenya responds to non-local upwelling events, specifically those that occur in the Arabian Sea during the SW monsoon. In comparison, water transported from the southern hemisphere subtropical gyre is responsible for seasonally elevated coral Δ^{14}C levels. The absence of a distinct sub-annual pre-bomb Δ^{14}C signal suggests that open and coastal upwelling are negligible off the coast of Kenya. In contrast, upwelled, depleted Δ^{14}C water from the coasts of Oman and Somalia is transported to the coast of Kenya via the wintertime SC during the NE monsoon. Our conclusion is supported by a negative lag relationship between the coral δ^{18}O and Δ^{14}C seasonal signal by 3–4 months as well model trajectory solutions.

Our results stand in contrast to previous work which suggests that the influence of monsoon-driven upwelling is propagated throughout the western Indian Ocean by the major current systems, especially the SEC. Southon *et al.* (2002) argue that the SEC, acting as a westward return flow, advects radiocarbon-depleted water to regions such as Mauritius, northern Madagascar and Seychelles via southeasterly flow from the Arabian Sea. In contrast to these sites, the Watamu coral site, slightly north of the SC and EACC confluence, is capturing the southward, upper-layer flow of the wintertime SC during the NE monsoon. Our findings show that the Watamu Δ^{14}C time-series behaves more like a subtropical site, reflecting a faster response time to atmospheric bomb input. We argue that the bomb peak would be delayed further if water was circulated in a basin-wide gyre.

Disparities between these records illustrates that a single $\Delta^{14}C$ coral record is not representative of the Indian Ocean as a whole in modeling uptake and distribution of bomb ^{14}C and documenting decadal variability. Thus, our coral radiocarbon record is the first to provide empirical evidence that return surface flow across the equator occurs at the western boundary. Whether this limb constitutes a significant portion of the Cross-equatorial Cell still needs to be validated. Nevertheless, we conclude that the role of the SC should be considered when addressing cross-equatorial return flow in the Indian Ocean.

REFERENCES

Bard, E., M. Arnold, G. Ostlund, H. P. Maurice, P. Monfray and J.-C. Duplessy. 1988. Penetration of bomb radiocarbon in the tropical Indian Ocean measured by means of accelerator mass spectrometry. Earth Planet. Sci. Lett., *87,* 379–389.

Broecker, W. S. and T.-S. Peng. 1982. Tracers in the Sea, Lamont-Doherty Geological Observatory, Columbia Univ., Palisades, NY, 690 pp.

Broecker, W. S., T.-S. Peng, G. Ostuland and M. Stuiver. 1985. The distribution of bomb radiocarbon in the ocean. J. Geophys. Res., *90,* 6953–6970.

Brown, T. A., G. W. Farwell, P. W. Grootes, F. H. Schmidt and M. Stuiver. 1993. Intra-annual variability of the radiocarbon content of corals from the Galapagos Islands. Radiocarbon, *35,* 245–251.

Conkright, M., S. Levitus, T. O'Brien, T. Boyer, J. Antonov and C. Stephens. 1998. World Ocean Atlas 1998 CD-ROM Data Set Documentation. Tech. Rep. 15, NODC Internal Report, Silver Spring, MD, 16 pp.

Coplen, T. B. 1994. Reporting of stable hydrogen, carbon, and oxygen isotopic abundances. Pure and Applied Chem., *66,* 273–276.

Dettinger, M. D., M. Ghil, C. M. Strong, W. Weibel and P. Yiou. 1995. Software expedites singular-spectrum analysis of noisy time series, Eos, Trans. American Geophysical Union, *76,* 12, 14, 21.

Druffel, E. M. 1982. Banded corals: Changes in oceanic ^{14}C during the Little Ice Age. Science, *218,* 13–19.

—— 1987. Bomb radiocarbon in the Pacific: Annual and seasonal timescale variations. J. Mar. Res., *45,* 667–698.

—— 1989. Decade time scale variability of ventilation in the North Atlantic: High precision measurements of bomb radiocarbon in banded corals. J. Geophys. Res., *94,* 3271–3285.

Druffel, E. M. and T. W. Linick. 1978. Radiocarbon in annual coral rings of Florida. Geophys. Res. Lett., *5,* 913–916.

Druffel, E. M. and H. E. Suess. 1983. On the radiocarbon record in banded corals: Exchange

parameters and net transport of $^{14}CO_2$ between atmosphere and surface ocean. J. Geophys. Res., *88,* 1271–1280.

Duing, W. and F. Schott. 1978. Measurements in the source region of the Somali Current during the Monsoon reversal. J. Phys. Oceanogr., *8,* 278–289.

Fischer, J., F. Schott and L. Stramma. 1996. Currents and transports of the Great Whirl Socotra Gyre system during the summer monsoon August 1993. J. Geophys. Res., *101,* 3573–3587.

Goyet, C., C. Coatanoan, G. Eischeid, T. Amaoka, K. Okuda, R. Healy and S. Tsunogai. 1999. Spatial variation of total CO_2 and total alkalinity in the northern Indian Ocean: A novel approach for the quantification of anthropogenic CO_2 in seawater. J. Mar. Res., *57,* 135–163.

Grumet, N. S., R. B. Dunbar and J. E. Cole. 2001. Multisite record of climate change from Indian Ocean corals. Proceedings of the 9th International Coral Reef Symposium. 9th International Coral Reef Symposium, Bali, Indonesia. (in press).

Grumet, N. S., T. P. Guilderson and R. B. Dunbar. 2002. Pre-bomb radiocarbon variability inferred from a Kenyan coral record. Radiocarbon, (in press).

Guilderson, T. P. and D. P. Schrag. 1998. Abrupt shift in subsurface temperatures in the tropical Pacific associated with changes in El Nino. Science, *281,* 240–243.

Guilderson, T. P., D. P. Schrag, M. Kashgarian and J. Southon. 1998. Radiocarbon variability in the western equatorial Pacific inferred from a high-resolution coral record from Nauru Island. J. Geophys. Res., *103,* 24,641–24,650.

Guilderson, T. P., D. P. Schrag, E. Goddard, M. Kashgarian, G. Wellington and B. K. Linsley. 2000. Southwest subtropical Pacific surface water in a high-resolution coral record. Radiocarbon, *42,* 249–256.

Highsmith, R. C. 1979. Coral growth-rates and environmental-control of density banding. J. Exper. Mar. Bio. Ecol., *37,* 105–125.

Ishida, A., Y. Kashino, H. Mitsudera, N. Yoshioka and T. Kadokura. 1998. Preliminary results of a global high-resolution GCM experiment. J. Faculty Sci. Hokkaido Univ., Ser. VII 1, 441–460.

Jenkins, W. J. 1996. Studying thermocline ventilation and circulation using tritium and ^{3}He. Maurice Ewing Symposium Application of Trace Substance Measurements to Oceanographic Problems. AGU, Washington, D.C.

Ji, Z. and M. E. Luther. 1999. Circulation and heat budget of the Indian Ocean in a numerical model. Ocean Modeling and Prediction Laboratory Report. No. 99-06-01. University of South Florida, FL.

Johnson, D. R., M. M. Nguli and E. J. Kimani. 1982. Response to annually reversing monsoon winds at the southern boundary of the Somali Current. Deep Sea Res. I, *29,* 1217–1227.

Karstensen, J. and D. Quadfasel. 2002. Water subducted into the Indian Ocean. Deep-Sea Res. II, *49,* 1441–1457.

Key, R. M. and P. D. Quay. 2002. U.S. WOCE Indian Ocean Survey, Final Report for radiocarbon, Ocean Tracers Laboratory, Tech. Rep. #02-1. 2002a. Atmospheric and Oceanic Sciences Program, Princeton Univ., Princeton, NJ.

Key, Robert M., Paul D. Quay, Peter Schlosser, A. P. McNichol, K. F. von Reden, Robert J. Schneider, Kathy L. Elder, Minze Stuiver and H. Göte Östlund. 2002. WOCE Radiocarbon IV, Pacific Ocean Results: P10, P13N, P14C, P18, P19 & S4P. Radiocarbon, *44,* 239–392.

Levitus, S. 1982. Climatological Atlas of the World Ocean, NOAA Prof. Pap. No. 13, U.S. Govt. Print. Office, Washington, D.C., 173 pp.

Luther, M. E. 1999. Interannual variability in the Somali Current 1954–1976. Nonlinear Analysis, *35,* 59–83.

Miyama, T., J. P. McCreary, T. G. Jensen and J. Loschnigg. 2002. Structure and dynamics of the Indian-Ocean Cross-Equatorial Cell. Deep Sea Res. II, (in press).

Murtugudde, R. G., S. R. Signorini, J. R. Christian, A. J. Busalacchi, C. R. McClain and J. Picaut.

1999. Ocean color variability of the tropical Indo-Pacific basin observed by SeaWiFS during 1997–1998. J. Geophys. Res., *104,* 18,351–18,366.

Nydal, R. 2000. Radiocarbon in the ocean. Radiocarbon, *42,* 81–98.

Ostlund, H. G. and C. Grall. 1991. Indian Ocean radiocarbon: Data from the INDIGO 1, 2, and 3 cruises. Oak Ridge National Laboratory, DOE, Oak Ridge, TN.

Rao, T. S. S. and R. C. Griffiths. 1998. Understanding the Indian Ocean. UNESCO, Paris, *187,* 422 pp.

Rhein, M., L. Stramma and U. Send. 1995. The Atlantic Deep Western Boundary Current: Water Masses and Transports Near the Equator. J. Geophys. Res., *100,* 2441–2457.

Rodgers, K. B., M. A. Cane and D. P. Schrag. 1997. Seasonal variability of sea surface $\Delta^{14}C$ in the equatorial Pacific in an ocean circulation model. J. Geophys. Res., *102,* 18,627–18,639.

Rodgers, K. B., D. P. Schrag, M. A. Cane and N. H. Naik. 2000. The bomb C-14 transient in the Pacific Ocean. Geophys. Res., *105,* 8489–8512.

Schott, F. A., M. Dengler and R. Schoenefeldt. 2002. The shallow overturning circulation of the Indian Ocean. Progr. Ocean., *53,* 57–103.

Schott, F. and J. Fischer. 2000. Winter monsoon circulation of the northern Arabian Sea and Somali Current. J. Geophys. Res., *105,* 6359–6376.

Schott, F. A. and J. P. McCreary. 2001. The monsoon circulation of the Indian Ocean. Progr. Ocean., *51,* 1–123.

Southon, J., M. Kashgarian, M. Fontugne, B. Metivier and W. W. S. Yim. 2002. Marine reservoir corrections for the Indian Ocean and Southeast Asia. Radiocarbon, *44,* 167–180.

Stuiver, M. and H. G. Ostlund. 1983. GEOSECS Indian Ocean and Mediterranean. Radiocarbon, *25,* 1–29.

Stuiver, M. and H. A. Polach. 1977. Discussion reporting of ^{14}C data. Radiocarbon, *19,* 355–363.

Swallow, J. C., M. Fieux and F. Schott. 1988. The boundary currents east and north of Madagascar, Part I: Geostrophic currents and transports. J. Geophys. Res., *93,* 4951–4962.

Toggweiler, J. R., K. Dixon and W. S. Broecker. 1991. The Peru upwelling and the ventilation of the South Pacific thermocline. J. Geophys. Res., *96,* 20,467–20,497.

Tomczak, M. and J. S. Godfrey. 1994. Regional Oceanography: An Introduction. Pergamon Press, Oxford, England. 422 pp.

Vautard, R., P. Yiou and M. Ghil. 1992. Singular-spectrum analysis: A toolkit for short, noisy chaotic signals. Physica D, *58,* 95–126.

Woodberry, K. E., M. E. Luther and J. J. O'Brien. 1989. The wind-driven seasonal circulation in the southern tropical Indian Ocean. J. Geophys. Res., *94,* 17,985–18,002.

Zhang, H. M. and L. D. Talley. 1998. Heat and buoyancy budgets and mixing rates in the upper thermocline of the Indian and global oceans. J. Phys. Oceanogr., *28,* 1961–1978.